5-2016

Intravital Microscopy of Tumor Oxygenation and Glycolytic Demand

Jesse D. Ivers
University of Arkansas, Fayetteville

Intravital microscopy of tumor oxygenation and glycolytic demand
Jesse D. Ivers
University of Arkansas, Fayetteville
May 2016

Abstract

There is growing concern about the over treatment of cancer because treatments are based primarily on tumor anatomy. In this study, we aim to begin the process of addressing that issue by developing an intravital technique for optically analyzing tumor biology. Two traits were identified as having significant importance in the aggression of a tumor, vascular oxygenation (SO_2) and glycolytic demand. Dorsal skin flap window chambers were implanted and 4T1 and 67NR cancer cells were injected to provide a tumor model for the development of this intravital quantification technique. This study provides a detailed protocol from instrumentation setup to surgical procedures to imaging methods as well as showing that optical techniques can be used to quantify SO_2 and glycolytic demand within various cell lines.

Introduction

Carcinogenesis is a multistep process resulting in the formation and growth of a tumor. This process involves the development of a phenotypic properties that will best suit the cancer's growth within the body. This selective development is described as somatic evolution, due to its similarity to Darwinian evolution.[1] Within cancer cells, a variety of these phenotypic changes have been observed. These alterations to the normal phenotype occur in a variety of intensities in different types of cancer. A couple phenotypic changes worth noting are the increased rate of aerobic glycolysis[1] and the increased secretion of pro-angiogenic growth factors.[2]

Glycolysis is begins with the lysing of glucose into pyruvate. From this point, it is then converted to the waste product, lactic acid. When oxygen is available in normal mammalian cells, glycolysis is inhibited to allow for the oxidation of pyruvate and produce more energy per molecule of glucose.[1] Without oxygen, glycolysis nets only two adenosine triphosphate molecules (ATP), while in the presence of oxygen, oxidative phosphorylation pathway produces up to 15 times that amount.[3] Despite this differences, it has been observed that cancer cells convert to a phenotype of unregulated glycolysis. While the advantage for cancer cells is not yet fully known, it has been suggested that this common cancer occurrence must present a growth advantage for the tumor.[1]

Angiogenesis, or the formation of blood vessels, is driven by the secretion of angiogenic growth factors. Within cells in the process of carcinogenesis, there is a shifting balance between the anti- and pro-angiogenic growth factors. The point at which this balance

shifts in favor of the pro-angiogenic factors has been termed the “angiogenic switch.” This switch in cancer cells has clear somatic evolutionary value for the tumor. By initiating the formation of new vessels, a tumor can transition from being a dormant mass to a malignant outgrowth.[3]

While there are other aspects of carcinogenesis, these two have the potential to provide further inside into the development of a cancerous tumor and its aggressiveness. Having this insight could greatly improve the effectiveness and efficiency of cancer treatment. Usually, the three main courses of treatment include surgery, radiation, and chemotherapy. Each of these may be used separately or in conjunction with other treatments. Currently, the treatment of cancer is based primarily on tumor anatomy, including the cell type and the location. This information, while useful, is often not sufficient for selecting the most appropriate treatment plan.[4] In fact, the current standard of care often results in over-diagnosis leading to over-treatment of cancer. This means, cancer that may have been asymptomatic for a lifetime will be treated exposing the patient to undesirable side-effects.[5] These side-effects can include bleeding or clotting problems, fatigue, nausea and vomiting, and infertility.[6] It is clear that these effects will reduce a patients quality of life and any unnecessary exposure to them should be minimized.

In order to do that, treatment needs to center around tumor biology rather than anatomy. This requires an increased ability to understand the unique biology of a tumor and the cells comprising it. In order to determine this, different properties can be observed. For example, the ratio of NADH to FAD (redox ratio), two important molecules in oxidative

phosphorylation, has been used to differentiate between distinct cell lines based on their metabolisms *in vitro*. In this example, fluorescence confocal microscopy was used to exploit and quantify the endogenous fluorophores within cells.[7]

Additionally, a previous study established the ability to image vascular oxygenation (SO_2) of hemoglobin using only endogenous properties.[8] The method here is similar to that of pulse oximetry. Pulse oximetry technology quantifies oxygenation by the analysis of ratio of oxygenated hemoglobin (HbO_2) to total hemoglobin (Hb). This ratio is determined once again exploiting the endogenous electromagnetic phenomenon within the body. HbO_2 and deoxygenated hemoglobin (dHb) absorb light at distinct

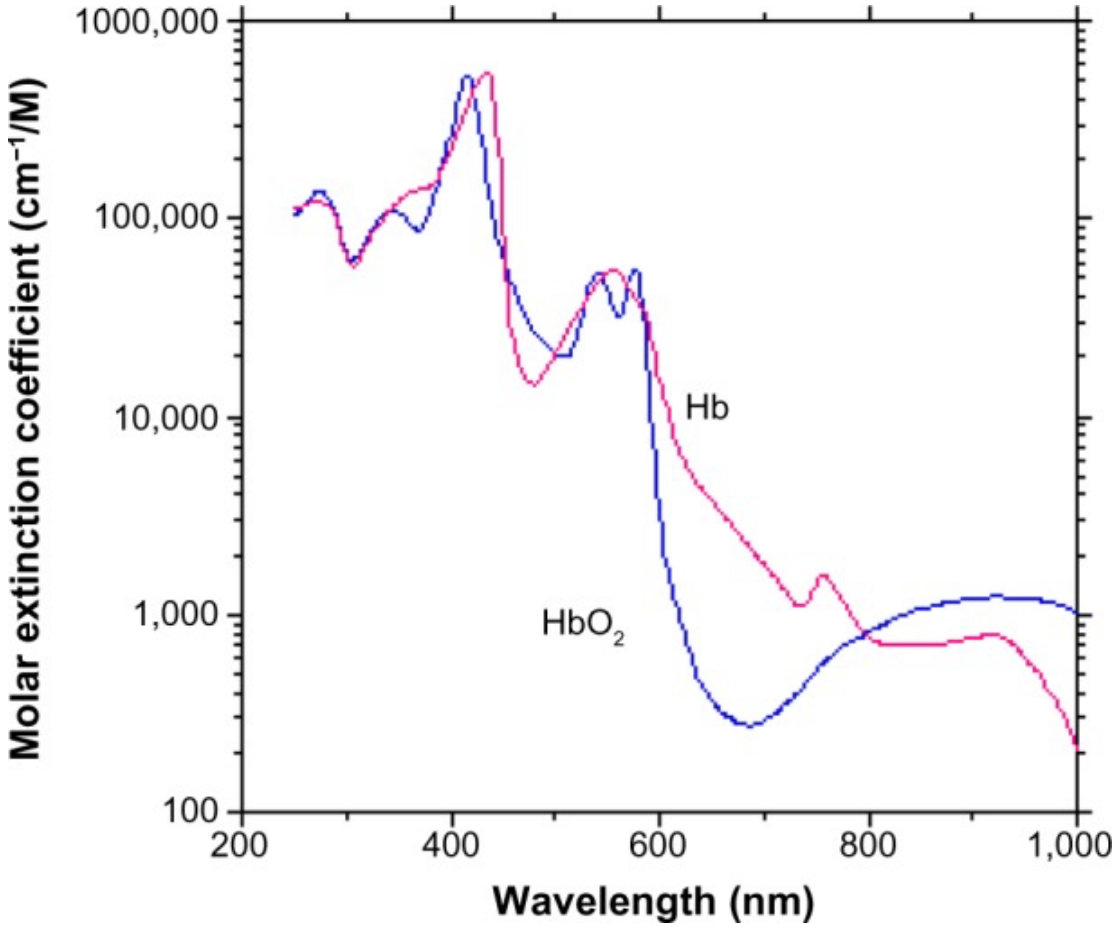

Figure 1 — Absorption spectra of the oxygenated and deoxygenated hemoglobin molecules.[9]

wavelengths as shown in Figure 1. Pulse oximetry uses this difference to quantify the presence of each molecule and determine the oxygenation saturation of the blood.[9]

Using the same principles as pulse oximetry, SO_2 can be determined within and surrounding an *in situ* tumor to quantify its angiogenic rate. Furthermore, 2-[N-(7-nitrobenz-2-oxa-1,3-diaxol-4- yl)amino]-2-deoxyglucose (2-NBDG) may be used as a glucose analog to analyze the uptake of glucose within a tumor in order to quantify glycolytic demand in a similar fashion to the redox ratio described previously.

These two innovations shed light on the ability to quantify cell phenotypes using the optical properties of various molecules. Also, as state previously, studies have shown the ability to differentiate cell lines using optics.[7] The combination of these ideas may give rise to a new method of cancer diagnosis and treatment determination.

Four sibling murine mammary adenocarcinoma cell lines have been identified as having a spectrum of abilities concerning metastatic phases. These cell lines, 67NR, 168FARN, 4T07, and 4T01, are murine breast cancer cells. Each one has a different potential for metastasis (Table 1)[10]. Using dorsal skin flap window chambers to image glycolytic demand and SO_2,there is hope of identifying the optical profiles for each category of metastatic potential. This study aimed to develop an intravital microscopy protocol to

Cell Type	Primary Tumor	Intravasation	Extravasation	Metastatic Nodules
4T1	X	X	X	X
4T07	X	X	X	
168FARN	X	X		
67NR	X			

Table 1 — Adapted from data presented in a previous study.[10] The furthest sequential event achieved in the metastatic process by each of the cell lines listed.

quantify tumor oxygenation and glycolytic demand for future use in profiling various cell lines with the goal of optically differentiating cell lines *in vivo*.

Methods

In order to develop said intravital imaging protocol, there were three important aims to be accomplished. First, the imaging instrumentation had to be configured for this specific procedure. Once the instrumentation was set-up, the surgical protocol was refined which lead into the development of the imaging protocol. In this study, the overarching aim was to develop, optimize, and refine a protocol for intravital microscopy from instrumentation set-up to surgical procedures to imaging.

Instrumentation

At its base, the system in use was an motorized inverted fluorescence microscope, the Olympus IX-81. Attached to the microscope was a 100 watt halogen lamp for transmission microscopy, 100 watt mercury lamp used for epifluorescent microscopy, a control box and hand switch, and a sequence of modular attachments to facilitate the unique needs of this study (Figure 2). Those components, pictured below in Figure 3, include a reducer lens, a two-piece collimating adapter, a liquid crystal tunable filter (LCTF), and the CCD.

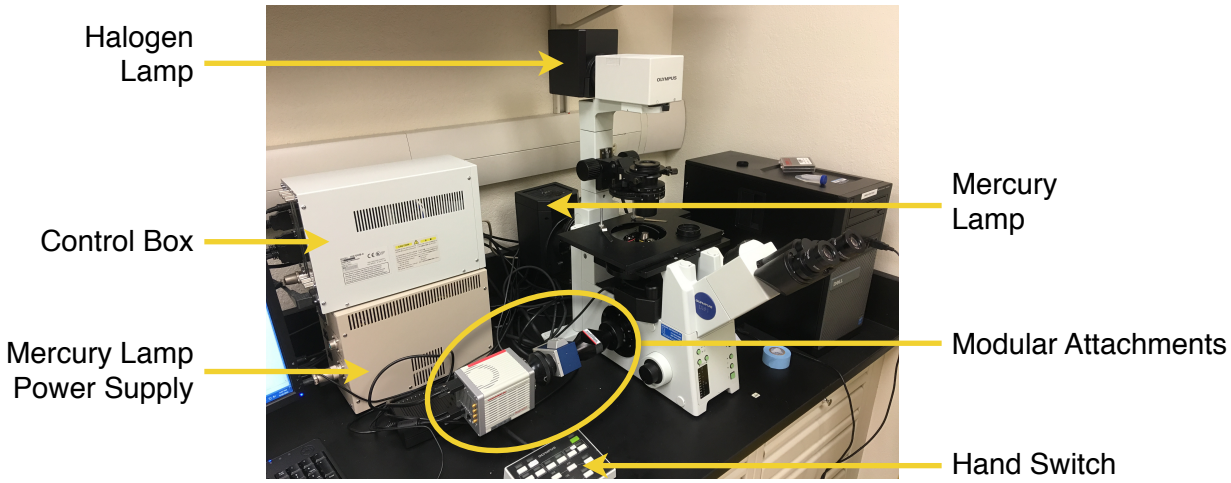

Figure 2 — The final microscope setup as used in this study with relevant labels.[11]

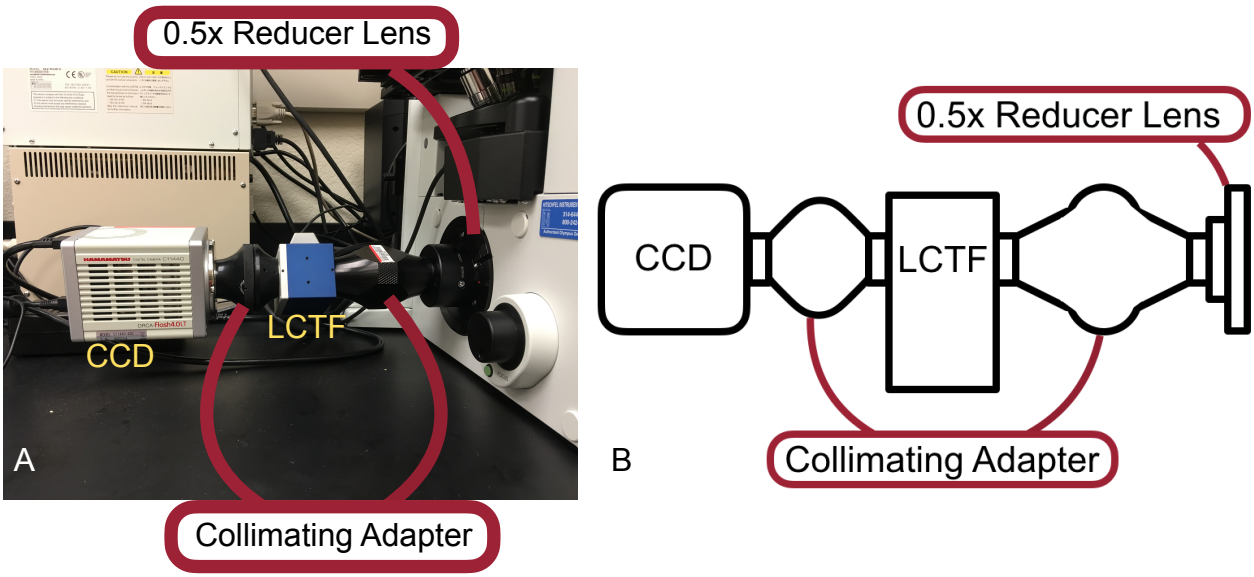

Figure 3 — **A.** Picture of modular attachments used in this study. **B.** A schematic of the attachments used.

Each of these components held a very specific purpose in this study. The LCTF was the firs addition to the system. A LCTF (VariSpec from CRi) allows for high-quality filtration of light transmission that can be rapidly controlled with high precision.[12] This filter would

be used in both transmission imaging for vascular oxygenation as well as reflective fluorescence for glycolytic demand.

Upon the addition of the LCTF, the tube length from the microscope to the CCD was altered, thus the image formed was no longer able to form on the CCD. This problem was resolved by the addition of the collimating adapter. The collimating adapter (XT-2 from Photometrics) creates infinity space between the two pieces. This infinity space allows fort the addition of optical components such as the LCTF. By adding components within the infinity space, the focal plane can be effortlessly realigned with the CCD sensor array and provide an in-focus image.[13]

Once the LCTF and collimating adapter were added, the platform became viable for the imaging desired. It as discovered, however, that the current field of view was not optimal for data collection. The field of view was too narrow, and thus a reducer lens was added to the system to increase the area imaged. The reducer lens was a simple 0.5x reducer lens added just prior to the first piece of the collimating adapter in the light path.

Finally, the CCD in use was in need of an update to allow better control, resolution, sensitivity, and speed. The original CCD in use was a Hamamatsu C4742-95. This CCD showed lack in the sensitivity and speed abilities. While it proved viable for transmission imaging, the low-intensity reflected fluorescence proved difficult to image without extreme integration times and high gains. Furthermore, the camera proved difficult to control through the computer. In order to solve these problems, a Hamamatsu C11440-42U. This CCD has a quantum efficiency of 70% at 600 nm. Also, it can image at 30 frames per second at full resolution, which is 2048x2048 effective pixels. The CCD

has a full well capacity of 30,000 electrons and a bit-depth of 16 bits. This CCD also helped improve the field of view of the imaging system.[14]

Surgical

The surgical procedures used in this study were adapted from a previous study.[15] To begin, the mouse is prepped for surgery being anesthetized with isoflurane gas and having its dorsal skin flap shaved of hair. After shaving, remaining hair is removed from the skin flap using hair removal cream. The mice used were female BALB/c mice for the convenience of care and housing. Upon surgical preparation, mice are anesthetized with approximately 100 μL 1:1:4 ketamine:xylazine:saline solution. Once anesthetized, an unbolted half of the chamber is used to mark points on the skin flap for bolts. Using a metal punch, the holes are punctured through the skin flap, being careful to avoid any organs. The bolted half of the chamber is then inserted through the three holes. The complimentary unbolted half is attached on the opposite side using three nuts.

Beneath the dermis is a fascial membrane. The procedure regarding this layer is the most delicate. Once the fascial layer is removed, cells are injected beneath the remaining facia. Following the injection of cells, the chamber is filled with sterile saline and a glass coverslip seals off the chamber. A lock ring is then used to hold the coverslip in the chamber. Once the window is sealed and secured, the skin flap is sutured to the upper edge of the window chamber following the guide holes.

The mouse is then allowed to recover from anesthesia and given a 100 µL subcutaneous Rhimadyl injection to alleviate pain. Once the mouse has fully recovered, it is returned to its cage.

The mice used underwent routine light-dark cycles and were allowed sufficient time for acclimation after arrival to our facility. Additionally, the entire surgical procedure is performed observing sterile techniques. A flow chart of the general procedure is shown in Figure 5.

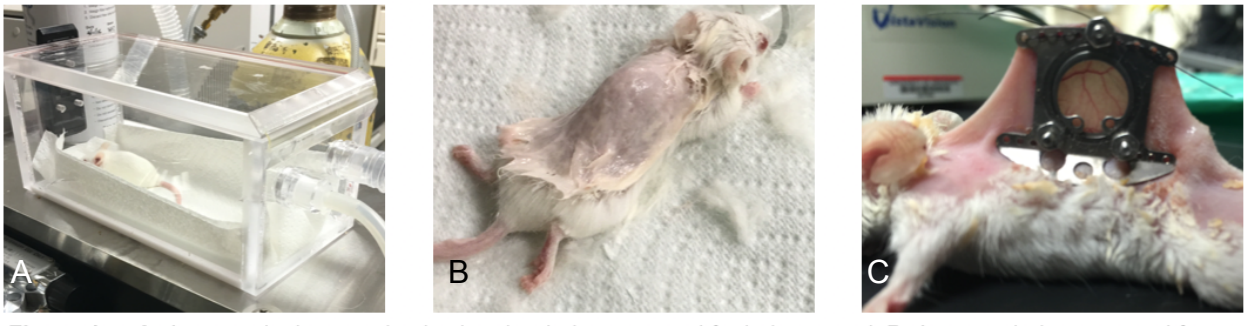

Figure 4 — **A**. A mouse in the anesthesia chamber being prepared for hair removal. **B**. A mouse being prepared for surgery. Mouse has just been shaven and hair-removal cream has been applied. **C**. A dorsal window chamber one day after implantation.

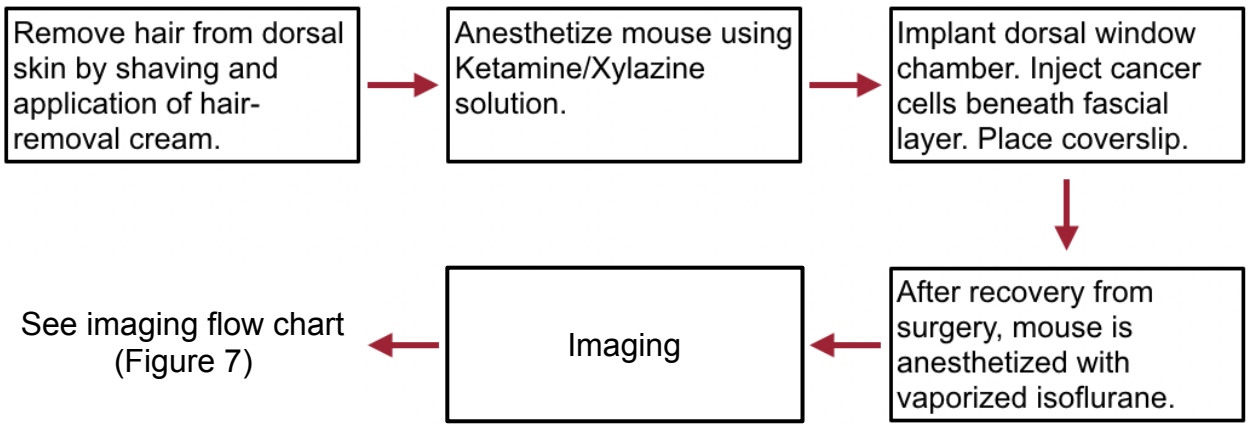

Figure 5 — Flow chart depicting the basic steps of the surgical procedure from preparation to recovery and imaging.

The cells used in this study were strategically selected to give both extremes of metastatic potential. They were selected from the four sibling lines described previously. In the final optimization, 6 mice were implanted with window chambers and injected with cells. Three were injected with 4T1 cells, highly metastatic, and three with 67NR, non-metastatic. Both sets of mice were then given sufficient time to develop a tumor for imaging.

Imaging

After the mice were given sufficient time to recover, at least 48 hours, the process of imaging could begin. Throughout the process of tumor development, SO_2 was observed in the mice. The instrumentation previously described was used for imaging of both SO_2 and glycolytic demand. Once tumors development was observed, glycolytic demand data would be collected. For the most precise identification of the relationship between SO_2, glycolytic demand, and metastatic potential, images for both phenotypes would be collected on the same day.

Before imaging could begin, mice were once again anesthetized in an isoflurane chamber. The window chamber was then fitted with a custom, 3D printed imaging platform (Figure 6A) to allow the securing of the mouse and window to the microscope stage. Once secure, an isoflurane nose cone was positioned over the nose of the mouse and used to keep the mouse anesthetized throughout the duration of imaging

(Figure 6B). The breathing rate was monitored to ensure no mouse was allowed to overdose on the isoflurane.

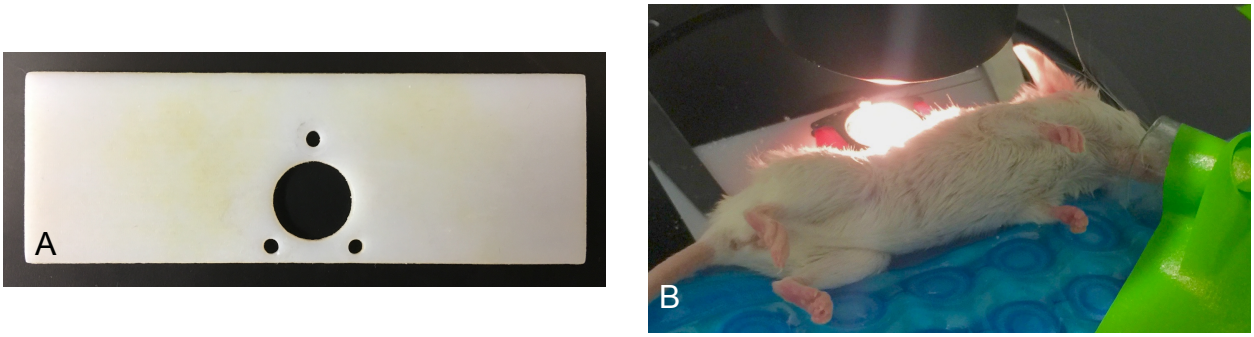

Figure 6 — **A**. Custom 3D printed imaging platform used to secure mice to stage of microscope. **B**. Mouse with imaging platform after being secured to microscope and nose cone positioned.

An imaging session would begin with the collection of SO_2 images. This process required the capture of eleven transmission images different wavelengths, 520nm - 620nm at 10nm increments. The LCTF was used to filter the transmitted light to these wavelengths. Due to the differential absorption of the tissue (as previously described in the discussion of hemoglobin), the intensity of transmission varied across the spectrum rather notably. In order to capture viable images despite this intensity variation, the integration time of the CCD was adjusted. Each session, the integration time used for each specific wavelength was carefully recorded. These times varied based on the tissue thickness of the mouse, and thus, a calibration was needed to ensure consistency across mice. In order to calibrate, a neutral density (ND) filter was imaged at the same specifications used for each mouse in each session. Also, a dark image

was taken where all light throughput from the microscope itself would be blocked before the objective. This was used to calibrate for any ambient light entering the system.

Once the SO_2 imaging was complete, the microscope would be switched to fluorescence mode by witching on the mercury lamp, closing the halogen lamp shutter, and aligning the appropriate filter cube. The tissue was excited at 470 nm and imaged at 535 nm, as was found in a previous sub-study to be the peak emission wavelength of 2-NBDG. Once the microscope was set-up for fluorescence, the mouse would be given a tail vein injection of 2-NBDG. Simultaneously, imaging would begin. Using Hamamatsu's HCImage software, an image sequence was programmed to semi-automate the following process of imaging. For the first 8 minutes, imaging was continuous at an integration time of 500-1000 ms (again, dependent on the tissue thickness). After the initial 8 minutes, images were taken every 1 minute until 30 total minutes had elapsed. Following that period, images were captured every 3 minutes until a total time of 75 minutes. All images were captured at the same integration time for a given mouse.

Lastly, the data received from imaging would be entered loaded a MATLAB program along with respective ND and dark images for analysis. This entire process is depicted in the flowchart below.

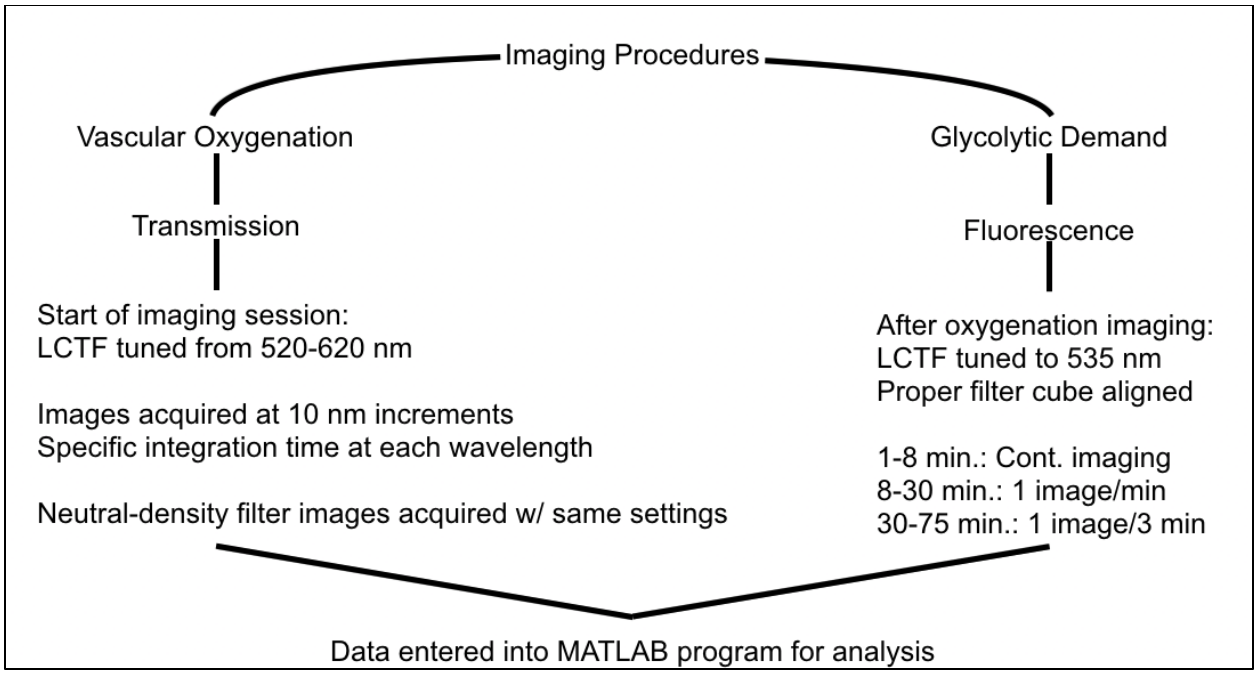

Figure 7 — Flow chart depicting the imaging processes for SO_2 and glycolytic demand.

Results and Discussion

In the final six mice at the conclusion and finalization of the protocol, the data showed that it is possible to quantify SO_2 and glycolytic demand *in vivo*. Furthermore, it is clear from the data (Figure 8) that distinctions can be made regarding the vascular oxygenation of different cell lines.

Unfortunately, in the collection of glycolytic demand data technical difficulties were experienced in regards to the storage of the data, thus only the 4T1 tumor was able to be analyzed (Figure 9).

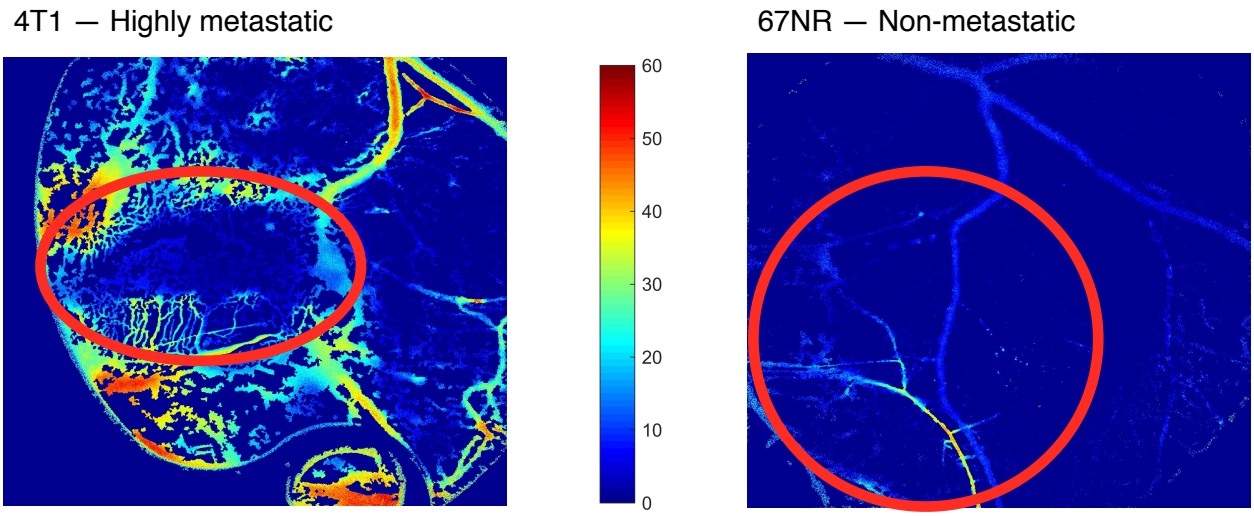

Figure 8 — Transmission images of SO_2 with suspicious areas highlighted with a red circle. **A**. 4T1 tumor 8 days after injection of cells. **B**. 67NR tumor 15 days after injection.

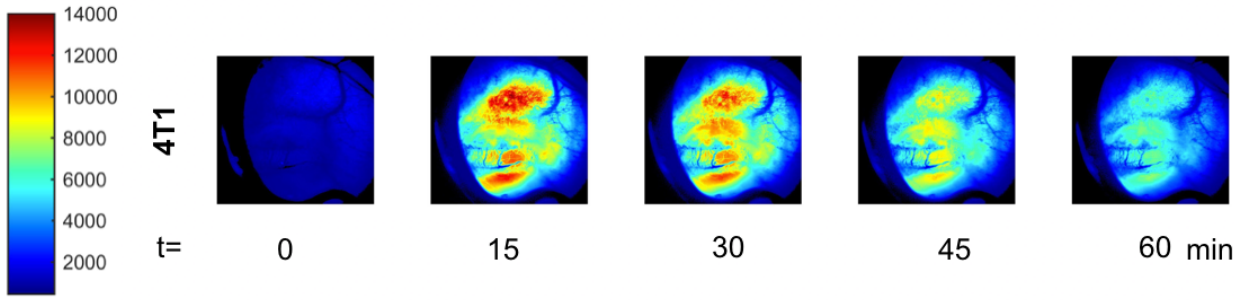

Figure 9 — *In vivo* uptake of 2-NBDG as quantification of glycolytic demand within 4T1 tumor and surrounding tissue.

Conclusions

From this study, it is clear that dorsal skin flap window chambers can be used to image and quantify *in vivo* vascular oxygenation and glycolytic demand. Furthermore, optical techniques can be used to identify the variations in these two phenotypes across cell

lines. Additionally, many significant conclusions were drawn about the optimization of the dorsal skin flap window chamber imaging protocol, as discussed above. Over the course of this study, there were several iterations of the protocol, resulting in the refining of the procedures and ultimately, the final protocol. Throughout this refining process, there were several resulting qualitative observations made on the optimal procedures and methods.

Throughout the multitude of surgical window implantations, it was discovered that the surgery should not be performed on any mouse with a mass less than 21 grams. When attempted, these mice showed increased tissue necrosis around the window, minimal tumor growth, and decreased quality of life. This is likely due to the excessive forces involved in stretching the less-abundant skin around the window chamber resulting in increased trauma. Another factor in successful recovery and tumor growth was the nut tightness. Originally, it was expected that the bolts would need to be fastened to firmly hold the two chamber halves together, but this most often resulted in tissue necrosis, as well. If the nuts were loosened in a timely manner, the necrosis could be prevented, though.

Another discovery regarding the nuts and bolts was the importance of directionality. Initially, the skin would be removed on the bolt-protrusion side. This would allow for an increased working distance on the inverted microscope. This increased the difficulty of the saline fill and coverslip and lock ring placement, though. Once the 3D printed platform was doubled in thickness, the added working distance was no longer necessary. Additionally, by changing which side to remove the skin, the future use of

two-photon microscopy in the window chambers was made possible, for now the protruding bolts will not hinder the close-proximity objective (Figure 4C).

A key observation in this study was the removing of the fascia. It was observed that if two much fascia was removed, the cells would not stay concentrated within the window and rarely a tumor would develop. If too much fascia was allowed to remain, though, images were rendered blurry and could not be used. In the final protocol, the outermost fascial layer is removed, but the inner most must be preserved in order to trap the cells to be injected within the window. This resulted in clear images while still having tumor growth (Figure 8, 9).

In order to begin to see tumors, approximately 10-20μL of cell solution would be injected in each mouse at about $5x10^6$ cells/mL. This was a dramatic increase from previous studies on athymic (nude) mice, which are immunocompromised.[16]

Future Direction

Using the developed protocol, cell lines of various metabolism, radiation susceptibility, angiogenic rate, and growth rate can be compared. With a further understanding of the relationship between SO_2 and glycolytic demand, and how each effects metastasis, the use of patient derived xenografts can be implemented for better understanding of the aggressions of specific tumor types. The hope being that treatment will become more specific, efficient, and effective as a result of this information.

References

1. Gatenby, R. A., & Gillies, R. J. (2004). Why do cancers have high aerobic glycolysis? Nature Reviews Cancer Nat Rev Cancer, 4(11), 891-899.

2. Baeriswyl, V., & Christofori, G. (2009). The angiogenic switch in carcinogenesis. Seminars in Cancer Biology, 19(5), 329-337. doi:10.1016/j.semcancer.2009.05.003

3. Embley, T. M., & Martin, W. (2006). Eukaryotic evolution, changes and challenges. Nature, 440(7084), 623-630. doi:10.1038/nature04546

4. How is Chemotherapy Used to Treat Cancer? (2016, February 16). Retrieved May 02, 2016, from http://www.cancer.org/treatment/treatmentsandsideeffects/treatmenttypes/chemotherapy/how-is-chemotherapy-used-to-treat-cancer

5. Marcus, P. M., Prorok, P. C., Miller, A. B., Devoto, E. J., & Kramer, B. S. (2015). Conceptualizing Overdiagnosis in Cancer Screening. JNCI Journal of the National Cancer Institute, 107(4). doi:10.1093/jnci/djv014

6. American Cancer Society. Cancer Treatment and Survivorship Facts & Figures 2014-2015. Atlanta: American Cancer Society; 2014

7. Ostrander, J. H., Mcmahon, C. M., Lem, S., Millon, S. R., Brown, J. Q., Seewaldt, V. L., & Ramanujam, N. (2010). Optical Redox Ratio Differentiates Breast Cancer Cell Lines Based on Estrogen Receptor Status. Cancer Research, 70(11), 4759-4766.

8. Sorg, B. S., Moeller, B. J., Donovan, O., Cao, Y., & Dewhirst, M. W. (2005). Hyperspectral imaging of hemoglobin saturation in tumor microvasculature and tumor hypoxia development. J. Biomed. Opt. Journal of Biomedical Optics, 10(4), 044004.

9. Nitzan, M., Romem, A., & Koppel, R. (2014). Pulse oximetry: Fundamentals and technology update. MDER Medical Devices: Evidence and Research, 231.

10. Miller, Fred R., and Cheryl J. Aslakson. "Selective Events in the Metastatic Process Defined by Analysis of the Sequential Dissemination of Subpopulations of a Mouse Mammary Tumor1." Cancer Research 52 (1992): 1399-405.

11. Olympus IX81 [PDF]. (n.d.). Center Valley, PA: Olympus.

12. Hensley, B., & Wyble, D. (2012). Spectral Imaging Using a Liquid Crystal Tunable Filter (Tech.). Rochester, NY: Mussel Color Science Lab.

13. Photometrics XT2TM Datasheet (Datasheet). (2013). Tuscon, AZ: Photometrics.

14. Hamamatsu Photonics. (2015). ORCA-Flash4.0LT [Brochure]. Bridgewater, NJ: Author.

15. Rajaram, N., Frees, A. E., Fontanella, A. N., Zhong, J., Hansen, K., Dewhirst, M. W., & Ramanujam, N. (2013). Delivery Rate Affects Uptake of a Fluorescent Glucose Analog in Murine Metastatic Breast Cancer. PLoS ONE, 8(10).

16. Zhong, J., Rajaram, N., Brizel, D. M., Frees, A. E., Ramanujam, N., Batinic-Haberle, I., & Dewhirst, M. W. (2013). Radiation induces aerobic glycolysis through reactive oxygen species. Radiotherapy and Oncology, 106(3), 390-396.

Acknowledgements

This study was performed under the guidance and mentorship of Dr. Narasimhan Rajaram and with the provision of materials through his laboratory. Andrew Briley assisted in this study. John Kennedy was responsible for the design and 3D printing of the imaging platform. Additional support was provided by the University of Arkansas Honors College Research Grant.